

Casimir interaction between spherical and planar plasma sheets

L. P. Teo*

*Department of Applied Mathematics, Faculty of Engineering, University of Nottingham Malaysia Campus,
Jalan Broga, 43500 Semenyih, Selangor Darul Ehsan, Malaysia*

(Received 2 March 2014; published 12 May 2014)

We consider the interaction between a spherical plasma sheet and a planar plasma sheet due to the vacuum fluctuations of electromagnetic fields. We derive the TGTG formula for the Casimir interaction energy and study its asymptotic behaviors. In the small separation regime, we confirm the proximity force approximation and calculate the first correction beyond the proximity force approximation. This study has potential application to model Casimir interaction between objects made of materials that can be modeled by plasma sheets such as graphene sheets.

DOI: [10.1103/PhysRevA.89.052509](https://doi.org/10.1103/PhysRevA.89.052509)

PACS number(s): 31.30.jh, 13.40.-f, 03.70.+k, 12.20.Ds

I. INTRODUCTION

Due to the potential impact to nanotechnology, the Casimir interactions between objects of nontrivial geometries have been under active research in recent years. Thanks to works done by several groups of researchers [1–14], we now have a formalism to compute the exact functional representation (known as the TGTG formula) for the Casimir interaction energy between two objects. Despite the seemingly different approaches taken, all the methods can be regarded as multiple scattering approaches, which can also be understood from the point of view of a mode summation approach [15–17]. The basic ingredients in the TGTG formula are the scattering matrices of the two objects and the translation matrices that relate the coordinate system of one object to the other. In the case that the objects have certain symmetries that allow a separable coordinate system to be employed, one can calculate these matrices explicitly. This has made possible the exact analytic and numerical analysis of the Casimir interaction between a sphere and a plate [18–29], between two spheres [30–32], between a cylinder and a plate [2,33,34], between two cylinders [35–38], between a sphere and a cylinder [39,40], as well as other geometries [41–43].

As is well known, the strength of the Casimir interaction not only depends on the geometries of the objects, it is also very sensitive to the boundary conditions imposed on the objects. For the past few years, many works have been done in the analysis of the quantum effect on objects with perfect boundary conditions such as Dirichlet, Neumann, perfectly conducting, infinitely permeable, etc. There are also a number of works which consider real materials such as metals modeled by plasma or Drude models [19,20,23–25,27,29,31,38,40]. In this work, we consider the Casimir interaction between a spherical plasma sheet and a planar plasma sheet. The plasma sheet model was considered in [33,44–49] to model a graphene sheet, describing the π electrons in C_{60} molecules. This model has its own appeal in describing a thin shell of materials that have the same attributes.

In [33], the Casimir interaction between a cylindrical plasma sheet and a planar plasma sheet has been considered. Our work can be considered as a generalization of [33] where

we consider a spherical plasma sheet instead of a cylindrical plasma sheet. One of the main objectives of the current work is to derive the TGTG formula for the Casimir interaction energy. As in [33], we are also going to study the asymptotic behaviors of the Casimir interaction in the small separation regime. We would expect that the leading term of the Casimir interaction coincides with the proximity force approximation (PFA), which we are going to confirm. Another major contribution would be the exact analytic computation of the next-to-leading order term which determines the deviation from PFA.

II. THE CASIMIR INTERACTION ENERGY

In this section, we derive the TGTG formula for the Casimir interaction energy between a spherical plasma sheet and a planar plasma sheet. We follow our approach in [17].

Assume that the spherical plasma sheet is a spherical surface of radius R and the planar plasma sheet is located at a distance L away from the center of the sphere.

The electromagnetic field is governed by the Maxwell equations:

$$\begin{aligned} \nabla \cdot \mathbf{E} &= \frac{\rho_f}{\epsilon_0}, & \nabla \times \mathbf{E} + \frac{\partial \mathbf{B}}{\partial t} &= \mathbf{0}, \\ \nabla \cdot \mathbf{B} &= 0, & \nabla \times \mathbf{B} - \frac{1}{c^2} \frac{\partial \mathbf{E}}{\partial t} &= \mu_0 \mathbf{J}_f. \end{aligned} \quad (1)$$

The free charge density ρ_f and free current density \mathbf{J}_f are functions having support on the plasma sheets (boundaries). The boundary conditions are given by [44]

$$\begin{aligned} \mathbf{E}_{|||S_+} - \mathbf{E}_{|||S_-} &= \mathbf{0}, \\ \mathbf{B}_n|_{S_+} - \mathbf{B}_n|_{S_-} &= 0, \\ \mathbf{E}_n|_{S_+} - \mathbf{E}_n|_{S_-} &= 2\Omega \frac{c^2}{\omega^2} \nabla_{||} \cdot \mathbf{E}_{|||S}, \\ \mathbf{B}_{|||S_+} - \mathbf{B}_{|||S_-} &= -2i\Omega \frac{1}{\omega} \mathbf{n} \times \mathbf{E}_{|||S}, \end{aligned} \quad (2)$$

where S is the boundary, S_+ and S_- are, respectively, the outside and inside of the boundary, \mathbf{n} is a unit vector normal to the boundary, and Ω is a constant characterizing the plasma, having dimension inverse of length.

Following the same scheme developed in [17], one can show that the Casimir interaction energy is given by the TGTG

*LeePeng.Teo@nottingham.edu.my

formula:

$$\begin{aligned} E_{\text{Cas}} &= \frac{\hbar}{2\pi} \int_0^\infty d\xi \text{Tr} \ln [\mathbb{I} - \mathbb{M}(i\xi)] \\ &= \frac{\hbar c}{2\pi} \int_0^\infty dk \text{Tr} \ln (\mathbb{I} - \mathbb{M}), \end{aligned} \quad (3)$$

where

$$\kappa = \frac{\xi}{c},$$

and the matrix \mathbb{M} can be written as

$$\mathbb{M} = \mathbb{T} \mathbb{V} \tilde{\mathbb{T}} \mathbb{W}.$$

In the work [11], the matrices \mathbb{V} and \mathbb{W} are written as \mathbb{G}_{12} and \mathbb{G}_{21} , and this is the origin of the name TGTG formula.

The matrices \mathbb{T} and $\tilde{\mathbb{T}}$ are obtained by matching boundary conditions (2) on the sphere and the plate, respectively. They are derived in the Appendix. The matrices \mathbb{V} and \mathbb{W} are translation matrices relating the spherical waves to planar waves and vice versa. They have been derived in [10,17].

Similar to the case of magnetodielectric sphere-plate configuration derived in [17], we then find that the components of the matrix \mathbb{M} , which are parametrized by $(lm, l'm')$ with $l, l' \geq 1$ and $-l \leq m \leq l$, $-l' \leq m' \leq l'$, are given by

$$\begin{aligned} \mathbb{M}_{lm, l'm'}(i\xi) &= \delta_{m, m'} \frac{(-1)^m \pi}{2} \sqrt{\frac{(2l+1)(2l'+1)}{l(l+1)l'(l'+1)}} \frac{(l-m)!(l'-m)!}{(l+m)!(l'+m)!} \mathbb{T}_{lm} \int_0^\infty d\theta \sinh \theta e^{-2\kappa L \cosh \theta} \\ &\times \begin{pmatrix} \sinh \theta P_l^{m'}(\cosh \theta) & -\frac{m}{\sinh \theta} P_l^m(\cosh \theta) \\ -\frac{m}{\sinh \theta} P_l^m(\cosh \theta) & \sinh \theta P_l^{m'}(\cosh \theta) \end{pmatrix} \begin{pmatrix} \frac{\Omega_p}{\Omega_p + \kappa \cosh \theta} & 0 \\ 0 & -\frac{\Omega_p \cosh \theta}{\Omega_p \cosh \theta + \kappa} \end{pmatrix} \\ &\times \begin{pmatrix} \sinh \theta P_{l'}^{m'}(\cosh \theta) & \frac{m'}{\sinh \theta} P_{l'}^{m'}(\cosh \theta) \\ \frac{m'}{\sinh \theta} P_{l'}^{m'}(\cosh \theta) & \sinh \theta P_{l'}^{m'}(\cosh \theta) \end{pmatrix}. \end{aligned} \quad (4)$$

Here $P_l^m(z)$ is an associated Legendre function and $P_l^{m'}(z)$ is its derivative, whereas \mathbb{T}_{lm} is a diagonal matrix:

$$\mathbb{T}_{lm} = \begin{pmatrix} T_{lm}^{\text{TE}} & 0 \\ 0 & T_{lm}^{\text{TM}} \end{pmatrix}$$

with

$$\begin{aligned} T_{lm}^{\text{TE}} &= \frac{2\Omega_s R I_{l+1/2}(\kappa R)^2}{1 + 2\Omega_s R I_{l+1/2}(\kappa R) K_{l+1/2}(\kappa R)}, \\ T_{lm}^{\text{TM}} &= -\frac{2\Omega_s \left[\frac{1}{2} I_{l+1/2}(\kappa R) + \kappa R I'_{l+1/2}(\kappa R) \right]^2}{\kappa^2 R - 2\Omega_s \left[\frac{1}{2} I_{l+1/2}(\kappa R) + \kappa R I'_{l+1/2}(\kappa R) \right] \left[\frac{1}{2} K_{l+1/2}(\kappa R) + \kappa R K'_{l+1/2}(\kappa R) \right]}. \end{aligned} \quad (5)$$

Ω_s and Ω_p are, respectively, the plasma parameters of the sphere and the plate.

In the limit $\Omega_s \rightarrow \infty$ and $\Omega_p \rightarrow \infty$, we find from (5) and (4) that

$$T_{lm}^{\text{TE}}(i\xi) = \frac{I_{l+1/2}(\kappa R)}{K_{l+1/2}(\kappa R)}, \quad T_{lm}^{\text{TM}}(i\xi) = \frac{\frac{1}{2} I_{l+1/2}(\kappa R) + \kappa R I'_{l+1/2}(\kappa R)}{\frac{1}{2} K_{l+1/2}(\kappa R) + \kappa R K'_{l+1/2}(\kappa R)}, \quad (6)$$

$$\begin{aligned} \mathbb{M}_{lm, l'm'}(i\xi) &= \delta_{m, m'} \frac{(-1)^m \pi}{2} \sqrt{\frac{(2l+1)(2l'+1)}{l(l+1)l'(l'+1)}} \frac{(l-m)!(l'-m)!}{(l+m)!(l'+m)!} \mathbb{T}_{lm} \int_0^\infty d\theta \sinh \theta e^{-2\kappa L \cosh \theta} \\ &\times \begin{pmatrix} 1 & 0 \\ 0 & -1 \end{pmatrix} \begin{pmatrix} \sinh \theta P_l^{m'}(\cosh \theta) & \frac{m}{\sinh \theta} P_l^m(\cosh \theta) \\ \frac{m}{\sinh \theta} P_l^m(\cosh \theta) & \sinh \theta P_l^{m'}(\cosh \theta) \end{pmatrix} \begin{pmatrix} \sinh \theta P_{l'}^{m'}(\cosh \theta) & \frac{m'}{\sinh \theta} P_{l'}^{m'}(\cosh \theta) \\ \frac{m'}{\sinh \theta} P_{l'}^{m'}(\cosh \theta) & \sinh \theta P_{l'}^{m'}(\cosh \theta) \end{pmatrix}, \end{aligned}$$

which recovers the Casimir interaction energy between a perfectly conducting spherical shell and a perfectly conducting plane [10,17].

III. SMALL SEPARATION ASYMPTOTIC BEHAVIOR

In this section, we consider the asymptotic behavior of the Casimir interaction energy when $d \ll R$, where $d = L - R$ is the distance between the spherical plasma sheet and the planar

plasma sheet. Let

$$\varepsilon = \frac{d}{R}$$

be the dimensionless parameter, and we consider $\varepsilon \ll 1$. There are also another two length parameters in the problem: $1/\Omega_s$ and $1/\Omega_p$. Let

$$\varpi_s = \Omega_s d, \quad \varpi_p = \Omega_p d.$$

They are dimensionless and we assume that they have order 1, i.e.,

$$\varpi_s \sim 1, \quad \varpi_p \sim 1.$$

First we consider the proximity force approximation to the Casimir interaction energy, which approximates the Casimir interaction energy by summing the local Casimir energy density between two planes over the surfaces.

The Casimir interaction energy density between two planar plasma sheets with respective parameters Ω_1 and Ω_2 is given by the Lifshitz formula [50]:

$$\mathcal{E}_{\text{Cas}}^{\parallel}(d) = \frac{\hbar c}{4\pi^2} \int_0^\infty d\kappa \int_0^\infty dk_\perp k_\perp \left[\ln(1 - r_{\text{TE}}^{(1)} r_{\text{TE}}^{(2)} e^{-2d\sqrt{k_\perp^2 + \kappa^2}}) + \ln(1 - r_{\text{TM}}^{(1)} r_{\text{TM}}^{(2)} e^{-2d\sqrt{\kappa^2 + k_\perp^2}}) \right].$$

Here d is the distance between the two planar sheets:

$$r_{\text{TE}}^{(i)} = \frac{\Omega_i}{\Omega_i + \sqrt{\kappa^2 + k_\perp^2}},$$

$$r_{\text{TM}}^{(i)} = -\frac{\Omega_i \sqrt{\kappa^2 + k_\perp^2}}{\Omega_i \sqrt{\kappa^2 + k_\perp^2} + \kappa^2}$$

are nothing but the components of the $\mathbb{T}_2^{\mathbf{k}_\perp}$ given in (A2).

The proximity force approximation for the Casimir interaction energy between a sphere and a plate is then given by

$$\begin{aligned} E_{\text{Cas}}^{\text{PFA}} &= R^2 \int_0^{2\pi} d\phi \int_0^\pi d\theta \sin \theta \mathcal{E}_{\text{Cas}}^{\parallel}(L + R \cos \theta) \\ &\sim 2\pi R \int_d^\infty du \mathcal{E}_{\text{Cas}}^{\parallel}(u) \\ &= -\frac{\hbar c R}{2\pi} \int_0^\infty d\kappa \int_0^\infty dk_\perp k_\perp \int_d^\infty du \sum_{n=1}^\infty \frac{1}{n} ([r_{\text{TE}}^{(1)} r_{\text{TE}}^{(2)}]^n + [r_{\text{TM}}^{(1)} r_{\text{TM}}^{(2)}]^n) e^{-2un\sqrt{\kappa^2 + k_\perp^2}} \\ &= -\frac{\hbar c R}{4\pi} \int_0^\infty d\kappa \int_0^\infty dk_\perp \frac{k_\perp}{\sqrt{\kappa^2 + k_\perp^2}} \sum_{n=1}^\infty \frac{1}{n^2} ([r_{\text{TE}}^{(1)} r_{\text{TE}}^{(2)}]^n + [r_{\text{TM}}^{(1)} r_{\text{TM}}^{(2)}]^n) e^{-2dn\sqrt{\kappa^2 + k_\perp^2}} \\ &= -\frac{\hbar c R}{4\pi} \int_0^\infty d\kappa \int_0^\infty dk_\perp \frac{k_\perp}{\sqrt{\kappa^2 + k_\perp^2}} [\text{Li}_2(r_{\text{TE}}^{(1)} r_{\text{TE}}^{(2)} e^{-2d\sqrt{\kappa^2 + k_\perp^2}}) + \text{Li}_2(r_{\text{TM}}^{(1)} r_{\text{TM}}^{(2)} e^{-2d\sqrt{\kappa^2 + k_\perp^2}})] \\ &= -\frac{\hbar c R}{4\pi} \int_0^\infty dq \int_0^q d\kappa [\text{Li}_2(r_{\text{TE}}^{(1)} r_{\text{TE}}^{(2)} e^{-2dq}) + \text{Li}_2(r_{\text{TM}}^{(1)} r_{\text{TM}}^{(2)} e^{-2dq})]. \end{aligned}$$

Here $\text{Li}_2(z) = \sum_{n=1}^\infty \frac{z^n}{n^2}$ is a polylogarithm function of order 2. Making a change of variables $dq = t$ and $\kappa = q\sqrt{1 - \tau^2} = t\sqrt{1 - \tau^2}/d$, we finally obtain

$$E_{\text{Cas}}^{\text{PFA}} = -\frac{\hbar c R}{4\pi d^2} \int_0^\infty dt t \int_0^1 \frac{d\tau \tau}{\sqrt{1 - \tau^2}} [\text{Li}_2(r_{\text{TE}}^{(1)} r_{\text{TE}}^{(2)} e^{-2t}) + \text{Li}_2(r_{\text{TM}}^{(1)} r_{\text{TM}}^{(2)} e^{-2t})], \quad (7)$$

where

$$r_{\text{TE}}^{(i)} = \frac{\Omega_i}{\Omega_i + q} = \frac{\varpi_i}{\varpi_i + t},$$

$$r_{\text{TM}}^{(i)} = -\frac{\Omega_i q}{\Omega_i q + \kappa^2} = -\frac{\varpi_i}{\varpi_i + t(1 - \tau^2)}.$$

Next, we consider the small separation asymptotic behavior of the Casimir interaction energy up to the next-to-leading order term in ε from the functional representation (3). In [29], we have considered the small separation asymptotic expansion of the Casimir interaction between a magnetodielectric sphere and a magnetodielectric plane. Our present scenario is similar to the one considered in [29]. The major differences are the boundary conditions on the sphere and the plate that are encoded in the two matrices \mathbb{T}_{lm} and $\mathbb{T}_{\mathbf{k}_\perp}$. Hence, we do not repeat the calculations that have been presented in [29], but only present the final result and point out the differences.

The leading term and next-to-leading term of the Casimir interaction energy E_{Cas}^0 and E_{Cas}^1 are given, respectively, by

$$E_{\text{Cas}}^0 = -\frac{\hbar c R}{4\pi d^2} \sum_{s=0}^{\infty} \frac{1}{(s+1)^2} \int_0^{\infty} dt t \int_0^1 \frac{d\tau \tau}{\sqrt{1-\tau^2}} e^{-2t(s+1)} \sum_{*=TE,TM} [T_0^* \tilde{T}_0^*]^{s+1}, \quad (8)$$

$$E_{\text{Cas}}^1 = -\frac{\hbar c}{4\pi d} \sum_{s=0}^{\infty} \frac{1}{(s+1)^2} \int_0^{\infty} dt t \int_0^1 \frac{d\tau \tau}{\sqrt{1-\tau^2}} e^{-2t(s+1)} \left\{ \sum_{*=TE,TM} [T_0^* \tilde{T}_0^*]^{s+1} (\mathcal{A} + \mathcal{C}^* + \mathcal{D}^*) + \mathcal{B} \right\}. \quad (9)$$

Here

$$T_0^{\text{TE}} = \frac{\varpi_s}{\varpi_s + t},$$

$$T_0^{\text{TM}} = \frac{\varpi_s}{\varpi_s + t(1-\tau^2)},$$

$$\tilde{T}_0^{\text{TE}} = \frac{\varpi_p}{\varpi_p + t},$$

$$\tilde{T}_0^{\text{TM}} = \frac{\varpi_p}{\varpi_p + t(1-\tau^2)},$$

$$\begin{aligned} \mathcal{A} &= \frac{t\tau^2}{3}[(s+1)^3 + 2(s+1)] + \frac{1}{3}[(\tau^2 - 2)(s+1)^2 - 3\tau(s+1) + 2\tau^2 - 1] \\ &\quad + \frac{\tau^4 + \tau^2 - 12}{12t\tau^2}(s+1) + \frac{(1+\tau)(1-\tau^2)}{2t\tau^2} - \frac{(1-\tau^2)}{3t} \frac{1}{s+1}, \end{aligned}$$

$$\mathcal{B} = \frac{1-\tau^2}{2t\tau^2} \left\{ (T_0^{\text{TE}} \tilde{T}_0^{\text{TM}} + T_0^{\text{TM}} \tilde{T}_0^{\text{TE}}) \frac{[T_0^{\text{TE}} \tilde{T}_0^{\text{TE}}]^{s+1} - [T_0^{\text{TM}} \tilde{T}_0^{\text{TM}}]^{s+1}}{T_0^{\text{TE}} \tilde{T}_0^{\text{TE}} - T_0^{\text{TM}} \tilde{T}_0^{\text{TM}}} + 2T_0^{\text{TE}} \tilde{T}_0^{\text{TE}} T_0^{\text{TM}} \tilde{T}_0^{\text{TM}} \frac{[T_0^{\text{TE}} \tilde{T}_0^{\text{TE}}]^s - [T_0^{\text{TM}} \tilde{T}_0^{\text{TM}}]^s}{T_0^{\text{TE}} \tilde{T}_0^{\text{TE}} - T_0^{\text{TM}} \tilde{T}_0^{\text{TM}}} \right\},$$

$$\mathcal{C}^* = C_V \mathcal{K}_1^* + C_J \mathcal{W}_1^*,$$

$$\mathcal{D}^* = D_{VV} \mathcal{K}_1^{*2} + D_{VJ} \mathcal{K}_1^* \mathcal{W}_1^* + D_{JJ} \mathcal{W}_1^{*2} + D_V \mathcal{K}_2^* + D_J \mathcal{W}_2^* + (s+1) \mathcal{Y}_2^*,$$

with

$$\begin{aligned} C_V &= -\frac{\tau}{3}[(s+1)^3 + 2(s+1)] + \frac{1-\tau^2}{6t\tau}(s+1)^2 \\ &\quad + \frac{1}{2t}(s+1) + \frac{1-4\tau^2}{12t\tau}, \end{aligned}$$

$$C_J = -\frac{t\tau}{3}[(s+1)^3 - (s+1)] + \frac{1}{6\tau}[(s+1)^2 - 1],$$

$$D_{VV} = \frac{1}{12t}[(s+1)^3 - 2(s+1)^2 + 2(s+1) - 1],$$

$$D_{JJ} = \frac{t}{12}[(s+1)^3 - 2(s+1)^2 - (s+1) + 2],$$

$$D_{VJ} = \frac{1}{6}[(s+1)^3 - (s+1)],$$

$$D_V = \frac{1}{6t}[2(s+1)^2 + 1],$$

$$D_J = \frac{t}{3}[(s+1)^2 - 1],$$

$$\mathcal{K}_1^{\text{TE}} = -\frac{t\tau}{\varpi_p + t},$$

$$\mathcal{K}_2^{\text{TE}} = -\frac{t[\varpi_p + t(1-2\tau^2)]}{2(\varpi_p + t)^2},$$

$$\begin{aligned} \mathcal{K}_1^{\text{TM}} &= \frac{t(1-\tau^2)}{\varpi_p + t(1-\tau^2)}, \\ \mathcal{K}_2^{\text{TM}} &= \frac{t(1-\tau^2)[\varpi_p(1-2\tau^2) + t(1-\tau^2)]}{2(\varpi_p + t(1-\tau^2))^2}, \\ \mathcal{W}_1^{\text{TE}} &= -\frac{\tau}{\varpi_s + t}, \\ \mathcal{W}_2^{\text{TE}} &= -\frac{[t(1-3\tau^2) + \varpi_s(1-\tau^2)]}{2t(\varpi_s + t)^2}, \\ \mathcal{Y}_2^{\text{TE}} &= -\frac{\tau}{2(\varpi_s + t)} + \frac{1}{t} \left(\frac{1}{4} - \frac{5\tau^2}{12} \right), \\ \mathcal{W}_1^{\text{TM}} &= \frac{\tau(1-\tau^2)}{\varpi_s + t(1-\tau^2)}, \\ \mathcal{W}_2^{\text{TM}} &= \frac{(1-\tau^2)[t(1-\tau^2)^2 + \varpi_s(1-3\tau^2)]}{2t[\varpi_s + t(1-\tau^2)]^2}, \\ \mathcal{Y}_2^{\text{TM}} &= \frac{\tau(1-\tau^2)}{2[\varpi_s + t(1-\tau^2)]} + \frac{1}{t} \left(\frac{1}{4} + \frac{7\tau^2}{12} \right). \end{aligned}$$

We have replaced the l in [29] with $t\tau/\varepsilon$. The definitions of \mathcal{B} , \mathcal{D} , C_V , C_J , D_{VV} , D_{VJ} , and D_{JJ} are slightly different than those in [29]. For $* = \text{TE}$ or TM , \mathcal{K}_1^* , \mathcal{K}_2^* , \mathcal{W}_1^* , \mathcal{W}_2^* , and \mathcal{Y}_2^* are obtained from the asymptotic expansions of \mathbb{T}_{lm} and $\tilde{\mathbb{T}}_{k_l}$. Hence, they are different than those obtained in [29].

Using polylogarithm function, we can rewrite the leading term E_{Cas}^0 (8) as

$$E_{\text{Cas}}^0 = -\frac{\hbar c R}{4\pi d^2} \int_0^\infty dt t \int_0^1 \frac{d\tau \tau}{\sqrt{1-\tau^2}} [\text{Li}_2(T_0^{\text{TE}} \tilde{T}_0^{\text{TE}} e^{-2t}) + \text{Li}_2(T_0^{\text{TM}} \tilde{T}_0^{\text{TM}} e^{-2t})]. \quad (10)$$

It is easy to see that this coincides with the proximity force approximation (7) when $\varpi_s = \varpi_1$ and $\varpi_p = \varpi_2$.

Notice that the leading term E_{Cas}^0 can be split into a sum of TE and TM contributions. However, because of the \mathcal{B} term, the next-to-leading order term E_{Cas}^1 (9) cannot be split into TE and TM contributions.

In the limit $\varpi_p, \varpi_s \rightarrow \infty$ which corresponds to perfectly conducting boundary conditions on the sphere and the plate, we find that for $* = \text{TE}$ or TM , $\mathcal{K}_1^*, \mathcal{K}_2^*, \mathcal{W}_1^*, \mathcal{W}_2^*$ vanishes, $T_0^* = \tilde{T}_0^* = 1$,

$$\begin{aligned} \mathcal{B} &= \frac{(1-\tau^2)}{2t\tau^2}(4s+2), \\ \mathcal{Y}_2^{\text{TE}} &= \frac{1}{t} \left(\frac{1}{4} - \frac{5\tau^2}{12} \right), \\ \mathcal{Y}_2^{\text{TM}} &= \frac{1}{t} \left(\frac{1}{4} + \frac{7\tau^2}{12} \right). \end{aligned}$$

Hence,

$$\begin{aligned} E_{\text{Cas}}^0 &= -\frac{\hbar c R}{2\pi d^2} \sum_{s=0}^{\infty} \frac{1}{(s+1)^2} \int_0^\infty dt t \int_0^1 \frac{d\tau \tau}{\sqrt{1-\tau^2}} e^{-2t(s+1)} \\ &= -\frac{\hbar c R}{8\pi d^2} \sum_{s=0}^{\infty} \frac{1}{(s+1)^4} \\ &= -\frac{\hbar c \pi^3 R}{720 d^2}, \\ E_{\text{Cas}}^1 &= -\frac{\hbar c}{4\pi d} \sum_{s=0}^{\infty} \frac{1}{(s+1)^2} \int_0^\infty dt t \int_0^1 \frac{d\tau \tau}{\sqrt{1-\tau^2}} e^{-2t(s+1)} \\ &\times [2\mathcal{A} + \mathcal{B} + (s+1)\mathcal{Y}_2^{\text{TE}} + (s+1)\mathcal{Y}_2^{\text{TM}}] \\ &= -\frac{\hbar c}{4\pi d} \sum_{s=0}^{\infty} \frac{1}{(s+1)^2} \left(\frac{1}{6(s+1)^2} - \frac{2}{3} \right) \\ &= E_{\text{Cas}}^0 \left(\frac{1}{3} - \frac{20}{\pi^2} \right) \frac{d}{R}. \end{aligned}$$

These recover the results for the case where both the sphere and the plane are perfectly conducting [26].

Next, we consider the special case where we have a spherical graphene sheet in front of a planar graphene sheet. The parameters Ω_s and Ω_p are both equal to $6.75 \times 10^5 \text{ m}^{-1}$ (see Ref. [50]). Assume that the radius of the spherical graphene sheet is $R = 1 \text{ mm}$. Let

$$E_{\text{Cas}}^{\text{PFA,PC}} = -\frac{\hbar c \pi^3 R}{720 d^2}$$

be the leading term of the Casimir interaction between a perfectly conducting sphere and a perfectly conducting plane. In Fig. 1, we plot the ratio of the leading term of the Casimir interaction energy E_{Cas}^0 to $E_{\text{Cas}}^{\text{PFA,PC}}$, and the ratio of the sum of the leading term and next-to-leading order term ($E_{\text{Cas}}^0 + E_{\text{Cas}}^1$) to $E_{\text{Cas}}^{\text{PFA,PC}}$. The ratio of $(E_{\text{Cas}}^0 + E_{\text{Cas}}^1)$ to E_{Cas}^0 is plotted in

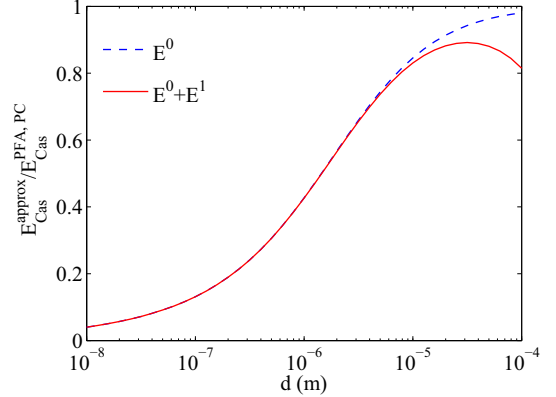


FIG. 1. (Color online) The leading order term of the Casimir interaction energy normalized by $E_{\text{Cas}}^{\text{PFA,PC}}$ (dashed line) and the sum of the leading and next-to-leading order terms normalized by $E_{\text{Cas}}^{\text{PFA,PC}}$ (solid line) in the case in which both the sphere and plane are graphene sheets.

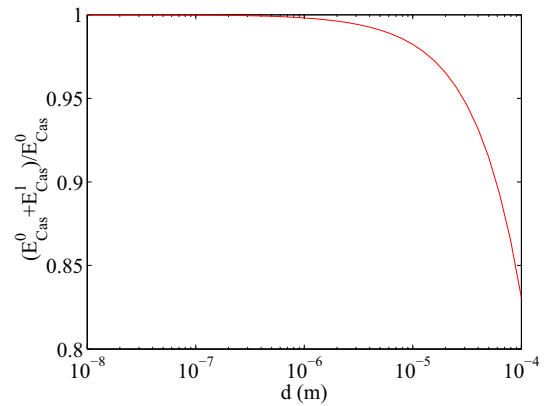


FIG. 2. (Color online) The ratio of the sum of the leading and next-to-leading order terms to the leading order term in the case in which both the sphere and plane are graphene sheets.

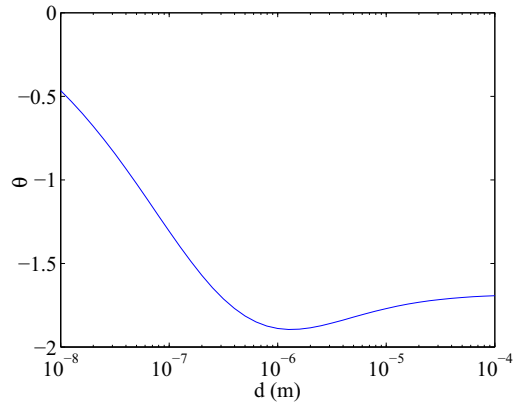


FIG. 3. (Color online) θ as a function of d in the case in which both the sphere and plane are graphene sheets.

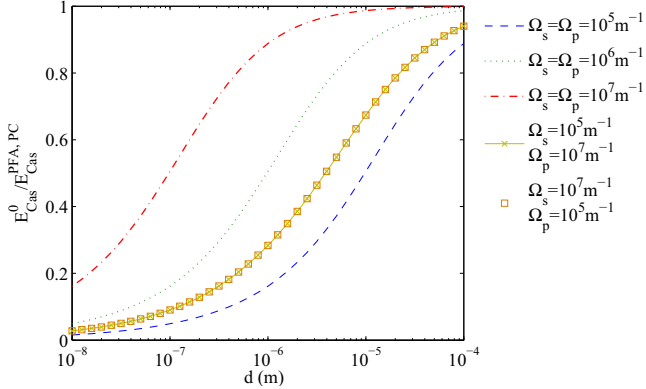
FIG. 4. (Color online) $E_{\text{Cas}}^0/E_{\text{Cas}}^{\text{PFA,PC}}$ as a function of d .

Fig. 2. From these graphs, we can see that the next-to-leading order term plays a significant correction role when $d/R \sim 0.1$.

Another important quantity that characterizes the correction to proximity force approximation is

$$\theta = \frac{E_{\text{Cas}}^1}{E_{\text{Cas}}^0} \frac{R}{d},$$

so that

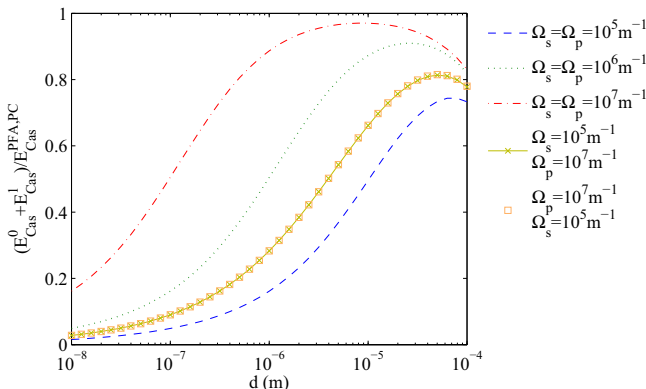
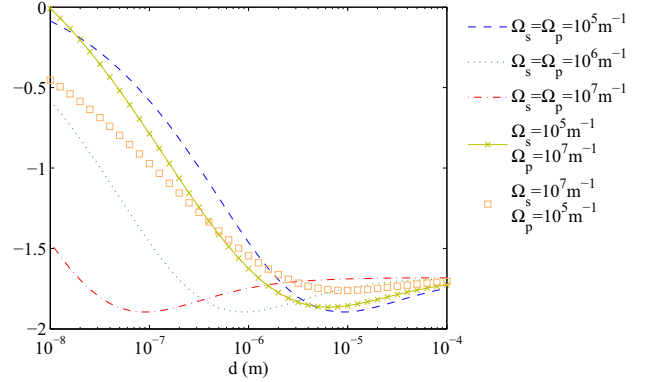
$$E_{\text{Cas}} = E_{\text{Cas}}^0 \left(1 + \frac{d}{R} \theta + \dots \right).$$

In the case of a perfectly conducting sphere and plane, θ is a pure number given by [26]

$$\theta = \frac{1}{3} - \frac{20}{\pi^2} = -1.69. \quad (11)$$

In Fig. 3, we plot θ as a function of d for a spherical graphene sheet in front of a planar graphene sheet. We observe that its variation pattern is significantly different from the case of a gold sphere and gold plane modeled by the plasma model and the Drude model which we studied in [29]. Nevertheless, as d is large enough, θ approaches the limiting value (11).

To study the dependence of the Casimir interaction energy on the parameters Ω_s and Ω_p , we plot in Figs. 4 and 5, respectively, the ratio $E_{\text{Cas}}^0/E_{\text{Cas}}^{\text{PFA,PC}}$ and the ratio $(E_{\text{Cas}}^0 + E_{\text{Cas}}^1)/E_{\text{Cas}}^{\text{PFA,PC}}$ as a function of d for various values of Ω_s and Ω_p . The variation of θ is plotted in Fig. 6. It is observed that the larger Ω , the larger the Casimir interaction energy.

FIG. 5. (Color online) $(E_{\text{Cas}}^0 + E_{\text{Cas}}^1)/E_{\text{Cas}}^{\text{PFA,PC}}$ as a function of d .FIG. 6. (Color online) θ as a function of d .

The behavior of θ shown in Fig. 6 is more interesting. It is observed that it has a minimum which appears at $d \sim \Omega^{-1}$ when $\Omega_s = \Omega_p = \Omega$.

IV. CONCLUSION

We study the Casimir interaction between a spherical object and a planar object that are made of materials that can be modeled as plasma sheets. The functional representation of the Casimir interaction energy is derived. It is then used to study the small separation asymptotic behavior of the Casimir interaction. The leading term of the Casimir interaction is confirmed to be in agreement with the proximity force approximation. The analytic formula for the next-to-leading order term is computed based on a previously established perturbation analysis [29]. The special case where the spherical object and planar object are graphene sheets is considered. The results are found to be quite different from the case of metallic sphere-plane configuration when the separation between the sphere and the plane is small. This may suggest a new experimental setup to test the Casimir effect. It also has potential application to nanotechnology.

ACKNOWLEDGMENTS

This work is supported by the Ministry of Higher Education of Malaysia under FRGS Grant No. FRGS/1/2013/ST02/UNIM/02/2. I would like to thank M. Bordag for proposing this question. I would also like to thank the anonymous referee for the helpful comments to improve the readability of this manuscript.

APPENDIX: DERIVATION OF THE \mathbb{T} AND $\tilde{\mathbb{T}}$ MATRICES

We assume that the center of the spherical plasma sheet is the origin and the planar plasma sheet is located at $z = L$.

Let \mathbf{A} be a vector potential that satisfies the gauge condition $\nabla \cdot \mathbf{A} = 0$ and such that

$$\mathbf{E} = -\frac{\partial \mathbf{A}}{\partial t}, \quad \mathbf{B} = \nabla \times \mathbf{A}.$$

Away from the boundaries, the solutions of the Maxwell equations (1) can be divided into transverse electric (TE) waves \mathbf{A}^{TE} and transverse magnetic (TM) waves \mathbf{A}^{TM} . They can be further divided into regular waves \mathbf{A}^{reg} that are regular at the

origin of the coordinate system and outgoing waves \mathbf{A}^{out} that decrease to zero rapidly when $\mathbf{x} \rightarrow \infty$ and k is replaced by ik . In rectangular coordinates, the waves are parametrized by $\mathbf{k}_\perp = (k_x, k_y) \in \mathbb{R}^2$, with

$$\begin{aligned}\mathbf{A}_{\mathbf{k}_\perp}^{\text{TE,reg}}(\mathbf{x}, t) &= \frac{1}{k_\perp} e^{ik_x x + ik_y y \mp i\sqrt{k^2 - k_\perp^2} z} (ik_y \mathbf{e}_x - ik_x \mathbf{e}_y) e^{-i\omega t}, \\ \mathbf{A}_{\mathbf{k}_\perp}^{\text{TM,reg}}(\mathbf{x}, t) &= \frac{1}{kk_\perp} e^{ik_x x + ik_y y \mp i\sqrt{k^2 - k_\perp^2} z} (\pm k_x \sqrt{k^2 - k_\perp^2} \mathbf{e}_x \pm k_y \sqrt{k^2 - k_\perp^2} \mathbf{e}_y + k_\perp^2 \mathbf{e}_z) e^{-i\omega t}.\end{aligned}$$

Here

$$k = \frac{\omega}{c}.$$

In spherical coordinates, the waves are parametrized by (l, m) , where $l = 1, 2, 3, \dots$ and $-l \leq m \leq l$, with

$$\begin{aligned}\mathbf{A}_{lm}^{\text{TE,*}}(\mathbf{x}, t) &= \frac{\mathcal{C}_l^*}{\sqrt{l(l+1)}} f_l^*(kr) \left(\frac{im}{\sin \theta} Y_{lm}(\theta, \phi) \mathbf{e}_\theta - \frac{\partial Y_{lm}(\theta, \phi)}{\partial \theta} \mathbf{e}_\phi \right) e^{-i\omega t}, \\ \mathbf{A}_{lm}^{\text{TM,*}}(\mathbf{x}, t) &= \mathcal{C}_l^* \left(\frac{\sqrt{l(l+1)}}{kr} f_l^*(kr) Y_{lm}(\theta, \phi) \mathbf{e}_r + \frac{1}{\sqrt{l(l+1)}} \frac{1}{kr} \frac{d}{dr} [rf_l^*(kr)] \left[\frac{\partial Y_{lm}(\theta, \phi)}{\partial \theta} \mathbf{e}_\theta + \frac{im}{\sin \theta} Y_{lm}(\theta, \phi) \mathbf{e}_\phi \right] \right) e^{-i\omega t}.\end{aligned}$$

Here $*$ = reg or out, with $f_l^{\text{reg}}(z) = j_l(z)$ and $f_l^{\text{out}}(z) = h_l^{(1)}(z)$, and $Y_{lm}(\theta, \phi)$ are the spherical harmonics. The constants $\mathcal{C}_l^{\text{reg}}$ and $\mathcal{C}_l^{\text{out}}$ are chosen so that

$$\mathcal{C}_l^{\text{reg}} j_l(i\zeta) = \sqrt{\frac{\pi}{2\zeta}} I_{l+1/2}(\zeta), \quad \mathcal{C}_l^{\text{out}} h_l^{(1)}(i\zeta) = \sqrt{\frac{\pi}{2\zeta}} K_{l+1/2}(\zeta).$$

To derive the \mathbb{T} matrix of the sphere, let

$$\mathbf{A}(\mathbf{x}, t) = A_1^{lm} \mathbf{A}_{lm}^{\text{TE,reg}}(\mathbf{x}, t) + C_1^{lm} \mathbf{A}_{lm}^{\text{TM,reg}}(\mathbf{x}, t)$$

inside the sphere and

$$\mathbf{A}(\mathbf{x}, t) = a_1^{lm} \mathbf{A}_{lm}^{\text{TE,reg}}(\mathbf{x}, \omega) + b_1^{lm} \mathbf{A}_{lm}^{\text{TE,out}}(\mathbf{x}, \omega) + c_1^{lm} \mathbf{A}_{lm}^{\text{TM,reg}}(\mathbf{x}, t) + d_1^{lm} \mathbf{A}_{lm}^{\text{TM,out}}(\mathbf{x}, t)$$

outside the sphere.

Let Ω_s be the parameter characterizing the spherical plasma sheet. Matching the boundary conditions (2) on the sphere gives

$$\begin{aligned}a_1^{lm} \mathcal{C}_l^{\text{reg}} j_l(kR) + b_1^{lm} \mathcal{C}_l^{\text{out}} h_l^{(1)}(kR) &= A_1^{lm} \mathcal{C}_l^{\text{reg}} j_l(kR), \\ a_1^{lm} \mathcal{C}_l^{\text{reg}} [j_l(kR) + kR j_l'(kR)] + b_1^{lm} \mathcal{C}_l^{\text{out}} [h_l^{(1)}(kR) + kR h_l^{(1)'}(kR)] - A_1^{lm} \mathcal{C}_l^{\text{reg}} [j_l(kR) + kR j_l'(kR)] &= 2\Omega_s R A_1^{lm} \mathcal{C}_l^{\text{reg}} j_l(kR), \\ c_1^{lm} \mathcal{C}_l^{\text{reg}} [j_l(kR) + kR j_l'(kR)] + d_1^{lm} \mathcal{C}_l^{\text{out}} [h_l^{(1)}(kR) + kR h_l^{(1)'}(kR)] &= C_1^{lm} \mathcal{C}_l^{\text{reg}} [j_l(kR) + kR j_l'(kR)], \\ c_1^{lm} \mathcal{C}_l^{\text{reg}} j_l(kR) + d_1^{lm} \mathcal{C}_l^{\text{out}} h_l^{(1)}(kR) - C_1^{lm} \mathcal{C}_l^{\text{reg}} j_l(kR) &= -\frac{2\Omega_s c^2}{\omega^2 R} C_1^{lm} \mathcal{C}_l^{\text{reg}} [j_l(kR) + kR j_l'(kR)].\end{aligned}$$

Eliminating A_1^{lm} and C_1^{lm} , we obtain a relation of the form

$$\begin{pmatrix} b_1^{lm} \\ d_1^{lm} \end{pmatrix} = -\mathbb{T}_{lm} \begin{pmatrix} a_1^{lm} \\ c_1^{lm} \end{pmatrix},$$

which defines the \mathbb{T} matrix. It is straightforward to show that \mathbb{T}_{lm} is a diagonal matrix:

$$\mathbb{T}_{lm} = \begin{pmatrix} T_{lm}^{\text{TE}} & 0 \\ 0 & T_{lm}^{\text{TM}} \end{pmatrix}$$

with

$$\begin{aligned}T_{lm}^{\text{TE}} &= \frac{2\Omega_s R I_{l+1/2}(kR)^2}{1 + 2\Omega_s R I_{l+1/2}(kR) K_{l+1/2}(kR)}, \\ T_{lm}^{\text{TM}} &= -\frac{2\Omega_s [\frac{1}{2} I_{l+1/2}(kR) + \kappa R I'_{l+1/2}(kR)]^2}{\kappa^2 R - 2\Omega_s [\frac{1}{2} I_{l+1/2}(kR) + \kappa R I'_{l+1/2}(kR)] [\frac{1}{2} K_{l+\frac{1}{2}}(kR) + \kappa R K'_{l+\frac{1}{2}}(kR)]}. \tag{A1}\end{aligned}$$

Here we have replaced k by $i\kappa$.

To derive the $\tilde{\mathbb{T}}$ matrix for the plane, let

$$\mathbf{A}(\mathbf{x}', t) = B_2^{\mathbf{k}_\perp} \mathbf{A}_{\mathbf{k}_\perp}^{\text{TE,out}}(\mathbf{x}', \omega) + D_2^{\mathbf{k}_\perp} \mathbf{A}_{\mathbf{k}_\perp}^{\text{TM,out}}(\mathbf{x}', \omega) e^{-i\omega t}$$

outside the plane ($z > L$), and

$$\mathbf{A}(\mathbf{x}', t) = a_2^{\mathbf{k}_\perp} \mathbf{A}_{\mathbf{k}_\perp}^{\text{TE,reg}}(\mathbf{x}', \omega) + b_2^{\mathbf{k}_\perp} \mathbf{A}_{\mathbf{k}_\perp}^{\text{TE,out}}(\mathbf{x}', \omega) + c_2^{\mathbf{k}_\perp} \mathbf{A}_{\mathbf{k}_\perp}^{\text{TM,reg}}(\mathbf{x}', \omega) + d_2^{\mathbf{k}_\perp} \mathbf{A}_{\mathbf{k}_\perp}^{\text{TM,out}}(\mathbf{x}', \omega) e^{-i\omega t}$$

inside the plane ($z < L$). Here $\mathbf{x}' = \mathbf{x} - \mathbf{L}$, where $\mathbf{L} = L\mathbf{e}_z$.

Denote by Ω_p the parameter characterizing the planar plasma sheet. Matching the boundary conditions (2) on the plane gives

$$\begin{aligned} a_2^{\mathbf{k}_\perp} + b_2^{\mathbf{k}_\perp} &= B_2^{\mathbf{k}_\perp}, \\ \sqrt{k^2 - k_\perp^2}(a_2^{\mathbf{k}_\perp} - b_2^{\mathbf{k}_\perp} + B_2^{\mathbf{k}_\perp}) &= -2i\Omega_p B_2^{\mathbf{k}_\perp}, \\ c_2^{\mathbf{k}_\perp} - d_2^{\mathbf{k}_\perp} &= -D_2^{\mathbf{k}_\perp}, \\ c_2^{\mathbf{k}_\perp} + d_2^{\mathbf{k}_\perp} - D_2^{\mathbf{k}_\perp} &= \frac{2i\Omega_p c^2}{\omega^2} \sqrt{k^2 - k_\perp^2} D_2^{\mathbf{k}_\perp}. \end{aligned}$$

From here, we find that we have a relation of the form

$$\begin{pmatrix} a_2^{\mathbf{k}_\perp} \\ c_2^{\mathbf{k}_\perp} \end{pmatrix} = -\tilde{\mathbb{T}}_{\mathbf{k}_\perp} \begin{pmatrix} b_2^{\mathbf{k}_\perp} \\ d_2^{\mathbf{k}_\perp} \end{pmatrix},$$

which defines the $\tilde{\mathbb{T}}$ matrix. $\tilde{\mathbb{T}}_{\mathbf{k}_\perp}$ is a diagonal matrix with elements

$$\tilde{T}_{\mathbf{k}_\perp}^{\text{TE}} = \frac{\Omega_p}{\Omega_p + \sqrt{k^2 + k_\perp^2}}, \quad \tilde{T}_{\mathbf{k}_\perp}^{\text{TM}} = -\frac{\Omega_p \sqrt{k^2 + k_\perp^2}}{\Omega_p \sqrt{k^2 + k_\perp^2} + \kappa^2}. \quad (\text{A2})$$

- [1] A. Bulgac, P. Magierski, and A. Wirzba, *Phys. Rev. D* **73**, 025007 (2006).
- [2] M. Bordag, *Phys. Rev. D* **73**, 125018 (2006).
- [3] A. Lambrecht, P. A. Maia Neto, and S. Reynaud, *New J. Phys.* **8**, 243 (2006).
- [4] T. Emig, R. L. Jaffe, M. Kardar, and A. Scardicchio, *Phys. Rev. Lett.* **96**, 080403 (2006).
- [5] S. J. Rahi, T. Emig, R. L. Jaffe, and M. Kardar, *Phys. Rev. A* **78**, 012104 (2008).
- [6] T. Emig, N. Graham, R. L. Jaffe, and M. Kardar, *Phys. Rev. Lett.* **99**, 170403 (2007).
- [7] T. Emig, N. Graham, R. L. Jaffe, and M. Kardar, *Phys. Rev. D* **77**, 025005 (2008).
- [8] T. Emig and R. L. Jaffe, *J. Phys. A: Math. Theor.* **41**, 164001 (2008).
- [9] T. Emig, *J. Stat. Mech.* (2008) P04007.
- [10] S. J. Rahi, T. Emig, N. Graham, R. L. Jaffe, and M. Kardar, *Phys. Rev. D* **80**, 085021 (2009).
- [11] O. Kenneth and I. Klich, *Phys. Rev. Lett.* **97**, 160401 (2006).
- [12] O. Kenneth and I. Klich, *Phys. Rev. B* **78**, 014103 (2008).
- [13] K. A. Milton and J. Wagner, *J. Phys. A: Math. Theor.* **41**, 155402 (2008).
- [14] K. A. Milton and J. Wagner, *Phys. Rev. D* **77**, 045005 (2008).
- [15] D. A. R. Dalvit, F. C. Lombardo, F. D. Mazzitelli, and R. Onofrio, *Phys. Rev. A* **74**, 020101(R) (2006).
- [16] F. D. Mazzitelli, D. A. R. Dalvit, and F. C. Lombardo, *New J. Phys.* **8**, 240 (2006).
- [17] L. P. Teo, *Int. J. Mod. Phys. A* **27**, 1230021 (2012).
- [18] M. Bordag and V. Nikolaev, *J. Phys. A: Math. Theor.* **41**, 164002 (2008).
- [19] A. Canaguier-Durand, P. A. Maia Neto, I. Cavero-Pelaez, A. Lambrecht, and S. Reynaud, *Phys. Rev. Lett.* **102**, 230404 (2009).
- [20] A. Canaguier-Durand, Paulo A. Maia Neto, A. Lambrecht, and S. Reynaud, *Phys. Rev. Lett.* **104**, 040403 (2010).
- [21] M. Bordag and V. Nikolaev, *Phys. Rev. D* **81**, 065011 (2010).
- [22] M. Bordag and I. Pirozhenko, *Phys. Rev. D* **81**, 085023 (2010).
- [23] R. Zandi, T. Emig, and U. Mohideen, *Phys. Rev. B* **81**, 195423 (2010).
- [24] A. Canaguier-Durand, P. A. Maia Neto, A. Lambrecht, and S. Reynaud, *Phys. Rev. A* **82**, 012511 (2010).
- [25] A. Canaguier-Durand, A. Gérardin, R. Guérout, P. A. Maia Neto, V. V. Nesvizhevsky, A. Y. Voronin, A. Lambrecht, and S. Reynaud, *Phys. Rev. A* **83**, 032508 (2011).
- [26] L. P. Teo, M. Bordag, and V. Nikolaev, *Phys. Rev. D* **84**, 125037 (2011).
- [27] A. Canaguier-Durand, G. L. Ingold, M. T. Jaekel, A. Lambrecht, Paulo A. Maia Neto, and S. Reynaud, *Phys. Rev. A* **85**, 052501 (2012).
- [28] I. G. Pirozhenko and M. Bordag, *Phys. Rev. D* **87**, 085031 (2013).
- [29] L. P. Teo, *Phys. Rev. D* **88**, 045019 (2013).
- [30] S. Zaheer, S. J. Rahi, T. Emig, and R. L. Jaffe, *Phys. Rev. A* **81**, 030502 (2010).

- [31] P. Rodriguez-Lopez, *Phys. Rev. B* **84**, 075431 (2011).
- [32] L. P. Teo, *Phys. Rev. D* **85**, 045027 (2012).
- [33] M. Bordag, *Phys. Rev. D* **75**, 065003 (2007).
- [34] L. P. Teo, *Phys. Rev. D* **84**, 025022 (2011).
- [35] F. C. Lombardo, F. D. Mazzitelli, and P. I. Villar, *J. Phys. A: Math. Theor.* **41**, 164009 (2008).
- [36] L. P. Teo, *Phys. Rev. D* **84**, 065027 (2011).
- [37] P. Rodriguez-Lopez and T. Emig, *Phys. Rev. A* **85**, 032510 (2012).
- [38] V. A. Golyk, M. Krüger, M. T. Homer Reid, and M. Kardar, *Phys. Rev. D* **85**, 065011 (2012).
- [39] L. P. Teo, *Phys. Rev. D* **87**, 045021 (2013).
- [40] E. Noruzifar, P. Rodriguez-Lopez, T. Emig, and R. Zandi, *Phys. Rev. A* **87**, 042504 (2013).
- [41] N. Graham, A. Shpunt, T. Emig, S. J. Rahi, R. L. Jaffe, and M. Kardar, *Phys. Rev. D* **81**, 061701 (2010).
- [42] N. Graham, A. Shpunt, T. Emig, S. J. Rahi, R. L. Jaffe, and M. Kardar, *Phys. Rev. D* **83**, 125007 (2011).
- [43] N. Graham, *Phys. Rev. D* **87**, 105004 (2013).
- [44] G. Barton, *J. Phys. A: Math. Gen.* **37**, 1011 (2004).
- [45] G. Barton, *J. Phys. A: Math. Gen.* **38**, 2997 (2005).
- [46] M. Bordag, *J. Phys. A: Math. Gen.* **39**, 6173 (2006).
- [47] M. Bordag and N. Khusnutdinov, *Phys. Rev. D* **77**, 085026 (2008).
- [48] N. R. Khusnutdinov, *Phys. Rev. B* **83**, 115454 (2011).
- [49] N. R. Khusnutdinov, *J. Phys. A* **45**, 265301 (2013).
- [50] M. Bordag, B. Geyer, G. L. Klimchitskaya, and V. M. Mostepanenko, *Phys. Rev. B* **74**, 205431 (2006).